Pulse

Research Article

Pulse 2024;12:95–105
DOI: 10.1159/000540666

Received: April 12, 2024
Accepted: July 28, 2024
Published online: July 31, 2024

# Validation of Noninvasive Derivation of the Central Aortic Pressure Waveform from Fingertip Photoplethysmography Using a Novel Selective Transfer Function Method

James R. Cox[a] Ehad Akeila[b] Alberto P. Avolio[a, b] Mark Butlin[a]
Catherine Liao[b] Gisele J. Bentley[a] Ahmad Qasem[a, b]

[a]Macquarie Medical School, Faculty of Medicine, Health and Human Sciences, Macquarie University, Sydney, NSW, Australia; [b]Cardiex Limited, Sydney, NSW, Australia



**Keywords**
Photoplethysmography · Transfer function · Waveform analysis · Aortic pressure · Blood pressure

**Abstract**

***Introduction:*** Central aortic pressure waveform analyses can provide clinically relevant information beyond conventional brachial blood pressure (BP) assessment. This waveform can be reproduced noninvasively through application of a generalized transfer function (GTF) on a peripheral waveform, as conventionally performed by applanation tonometry. Photoplethysmography (PPG) is an alternate approach; however, differences in measurement site and modality demand the use of a transfer function (TF) specific for those differences. This study aimed to compare central aortic waveform features generated from radial tonometry (reference) using a proprietary GTF with a central aortic waveform and its features generated from a simultaneous fingertip PPG measurement using a selective method where one of three different TFs is chosen based on the input signal harmonic profile. ***Methods:*** Brachial BP was measured in triplicate under resting conditions and was used for subsequent calibration. Multiple simultaneous radial tonometry (SphygmoCor CVMS) and fingertip PPG measurements were then performed in individual participants ($n$ = 21, 10 females, age: 39 ± 16 years). Measurements were converted into central aortic waveforms with their respective TFs. Twenty central aortic pressure waveform parameters were compared through correlation analysis, Bland-Altman plots, and a repeated measure mixed-effects ANOVA model. Central aortic waveform shape was compared using the root-mean-squared error (RMSE). ***Results:*** Correlation ($r$) of PPG-derived parameters with radially tonometry-derived central aortic parameters was high ranging from 0.79 to 0.99. Mean differences of pressure-related parameters were within 1.3 mm Hg, and differences of time-related parameters ranged from −2.2 to 3.4%. While some parameters were statistically different, these differences are not physiologically meaningful. Central aortic waveform shape had an average RMSE of 1.8 ± 0.9%. ***Conclusion:*** Fingertip PPG-derived central aortic waveform parameters using a novel selective TF were comparable to central aortic waveform features derived from radial tonometry using a previously validated GTF.



karger@karger.com
www.karger.com/pls



Correspondence to:
Ahmad Qasem, a.qasem@atcormedical.com

## Introduction

Traditionally, cardiovascular health is assessed from noninvasive brachial blood pressure (BP) measurements. Due to the pneumatic nature of the cuff, this only provides an intermittent estimation of brachial BP limited by measurement frequency which can also be uncomfortable and inconvenient for users. While brachial BP is a strong predictor of cardiovascular complications [1, 2], there is still a need to enhance the assessment of cardiovascular health beyond conventional BP values through more continuous and ambulatory assessment. This is especially true when considering the monitoring, management, and identification of health conditions, including but not limited to hypertension [3] or preeclampsia [4]. One potential solution to improving cardiovascular health evaluation is by analyzing the entire arterial waveform. The arterial waveform carries information that is reflective of the functionality of the cardiovascular system providing information on arterial stiffness [5] or oxygen supply and demand [6]. However, the arterial waveform varies in shape across the vasculature [7].

When considering the location of organs, measuring a central arterial waveform has the capacity to provide more clinically important information that could aid in the assessment of an individual's cardiovascular profile [8, 9]. Despite the complexities in measuring an invasive central waveform, a study by Chen et al. [10] validated the technique of noninvasively measuring a peripheral waveform and converting it to a central aortic waveform. This employs the use of a transfer function (TF) which has been adopted into technologies for central aortic pulse wave analysis (PWA), as implemented in the SphygmoCor CVMS/XCEL [11, 12], Complior [13], and Mobil-O-Graph [11], among others. The clinical relevance of PWA parameters from an array of sensor modalities has been highlighted in the literature [14, 15]. Attaining an arterial pulse waveform, regardless of the sensor modality, can enable continuous, or intermittent, pulse wave features to be measured.

Due to its near replication of the invasive radial BP waveform, a radial tonometric waveform has been historically the accepted noninvasive reference for acquiring a central arterial waveform using the mathematical application of a TF [16, 17]. Despite the high fidelity of radial tonometry, its measurement requires a degree of operator skill and can be considered inconvenient in an ambulatory environment. Brachial cuff volumetric displacement has also been used for waveform acquisition [18] but is limited in frequency of measurement and user-tolerance in an out-of-clinic environment [19]. Photoplethysmography (PPG), a technique using a small optical-based sensor, can provide a convenient and easy measure of the pulse waveform related to transient local changes in blood volume. The PPG waveform, typically

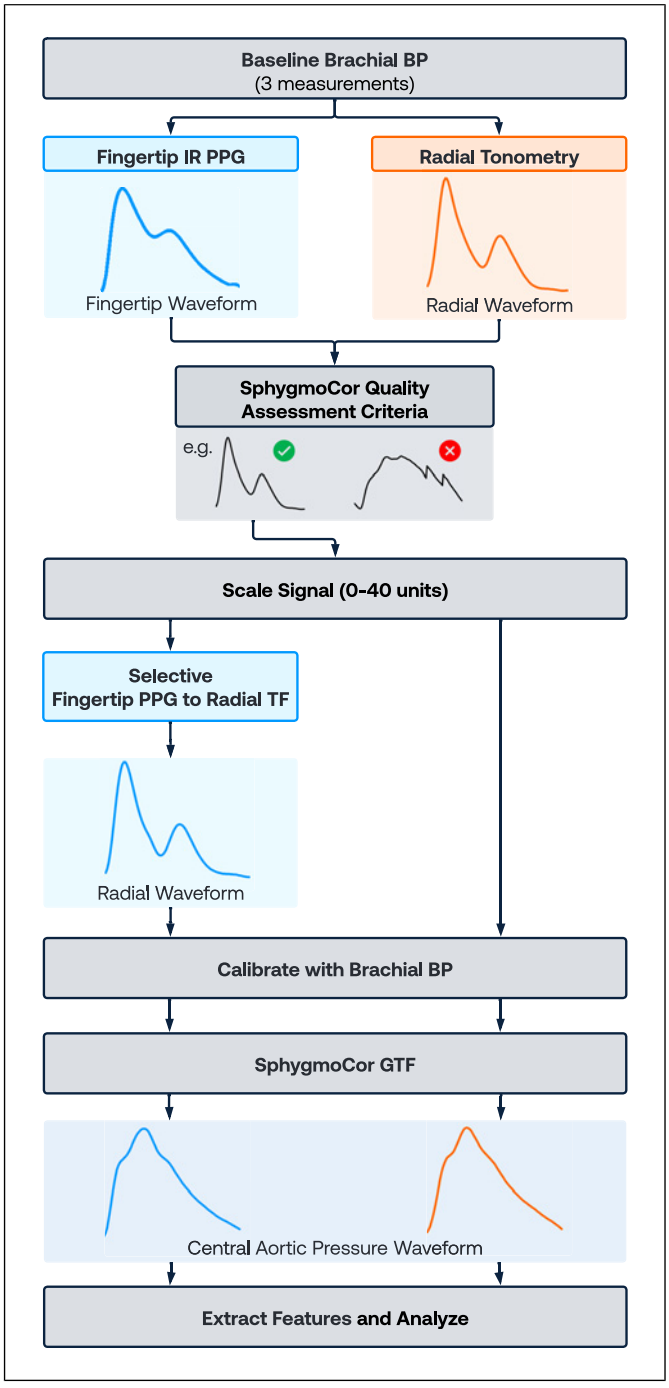


**Fig. 1.** Methodological flowchart. BP, blood pressure; IR PPG, infrared photoplethysmography; GTF, generalized transfer function; TF, transfer function.

measured in peripheral vascular beds, is generated from the change in absorbance of light synchronous with the pulsatile nature of the cardiac cycle and therefore provides a measure of local blood volume in the illuminated tissue [20]. This time-varying component produces a pulsatile waveform that varies within the cardiac cycle. However, published research on the use of PPG for central PWA is scarce. While other sensor modalities exist (e.g., ultrasound, radar) and may be used for the assessment of an arterial waveform, portability and expense of such modalities limit their use in an ambulatory setting. This research aims to compare central PWA parameters extracted from a radially acquired tonometric waveform using a proprietary generalized TF (GTF) with central PWA parameters acquired from a fingertip PPG waveform that uses a novel selective TF.

## Methods

A total of 21 participants (10 females, age: 39 ± 16 years) were recruited for the study. All participants provided written informed consent. Participants were excluded if they were pregnant, had arrhythmias, and/or had any other serious adverse cardiovascular complications. Ethics was reviewed and approved by the Institutional (Macquarie University) Human Research Ethics Committee (Ethics No: 52022911840017) and was conducted in accordance with the Declaration of Helsinki.

*Data Collection*

Participants underwent resting seated brachial oscillometric BP measurement in triplicate using the SphygmoCor XCEL (AtCor Medical, Sydney, Australia) on their right arm following at least 5 min of seated rest. Radial tonometry waveforms (SphygmoCor CVMS, AtCor Medical, Sydney, Australia) and fingertip infrared (IR) PPG (OSRAM BIOFY SFH 7072, ams-OSRAM AG, Premstätten, Austria) were then measured simultaneously for 13 s under resting baseline conditions on the same arm. A minimum of three and a maximum of five simultaneous tonometric and fingertip IR PPG measurements were collected per participant resulting in a total of 83 paired radial tonometric and fingertip IR PPG measurements. Radial and fingertip IR PPG signal quality was assessed by the SphygmoCor CVMS waveform quality control assessment which is based on pulse height, pulse height variations, and baseline drift. A total of 58 paired tonometric and PPG measurements remained, whereby each processed waveform was treated as an individual measurement. Figure 1 illustrates the methodological process.

*PPG TF Model Development*

A TF is the ratio of the harmonic amplitude and phase between the measured and the derived signals (shown in Fig. 2). The SphygmoCor device uses an invasively validated GTF that transforms a measured radial tonometry signal to a central aortic pressure pulse [10]. Given the differences in waveform shape between the radial tonometric waveform and a fingertip PPG waveform, the same TF cannot be applied to the fingertip PPG waveform. Therefore, a selection of TFs was generated to transform the fingertip PPG waveform into a radial artery pressure waveform, as detected by radial tonometry. From there, the radial to central aortic GTF could be applied to obtain the aortic waveform. The fingertip PPG to radial TF was calculated for each successful measurement ($n$ = 58). From the 58 successfully processed waveforms after performing a Fourier analysis, three different TFs were identified based on the harmonic profiles that best represented the variance across the range of harmonic profiles captured. The population study of central pressure waveforms covers all shapes, as described by Murgo et al. [21], whereby all central pressure waveform morphology is classified into three types based on impedance and systolic wave reflection profiles. As a result, 3 TFs covering all shapes were used in this algorithm. A propriety selective TF algorithm was developed to select the fingertip PPG signal to radial pulse TF based on the PPG signal harmonic profile of the first 5 harmonics. The fingertip PPG signal was converted to harmonics using fast Fourier transform, and depending on the harmonics (H0–H5) amplitude, a fingertip to radial pulse TF is selected (shown in Fig. 2).

The selection criteria employed by the novel selective TF were developed from three distinct measurements which came from three subjects. This method was then tested on the remaining 55 measurements, treated as individual measurements, to derive a radial waveform for each measurement, which was then converted to a central aortic pressure waveform using the GTF.

*Data Extraction*

Fingertip IR PPG waveforms scaled and were converted into radial waveforms using the selective TF (shown in Fig. 2), and then both the radial tonometric and fingertip IR PPG waveforms were calibrated with an average of the second and third brachial oscillometric BP measurements (systolic and diastolic) before the GTF was applied to attain a pressure-based aortic waveform. Central aortic waveforms and features from radial tonometry measurements were derived using the proprietary SphygmoCor GTF within the software (version V9; AtCor Medical, Sydney, Australia) and were extracted upon the completion of data collection. Conversion of the PPG fingertip waveform to radial then central waveforms and feature extraction was performed using a custom-written script in Python (version 3.11.2).

*Waveform Parameters*

Twenty parameters were calculated from the converted waveforms (illustrated in Fig. 3): central systolic blood pressure (cSBP: maximum central aortic pressure during systole); central diastolic blood pressure (cDBP: lowest central aortic pressure during diastole); central pulse pressure (pressure difference between cSBP and cDBP); central augmentation pressure (the difference between the peak pressure of the forward traveling wave generated during cardiac ejection [P1] and the reflected traveling wave caused by impedance mismatch [P2]); central augmentation index (cAIx: a ratio of AP to PP); cAIx corrected to a heart rate (HR) of 75 beats per minute [22]; subendocardial viability ratio (SEVR: a ratio of diastolic time index to TTI reflective of myocardial supply and demand); pulse pressure amplification (pulse pressure amplification: pulse pressure amplification from the

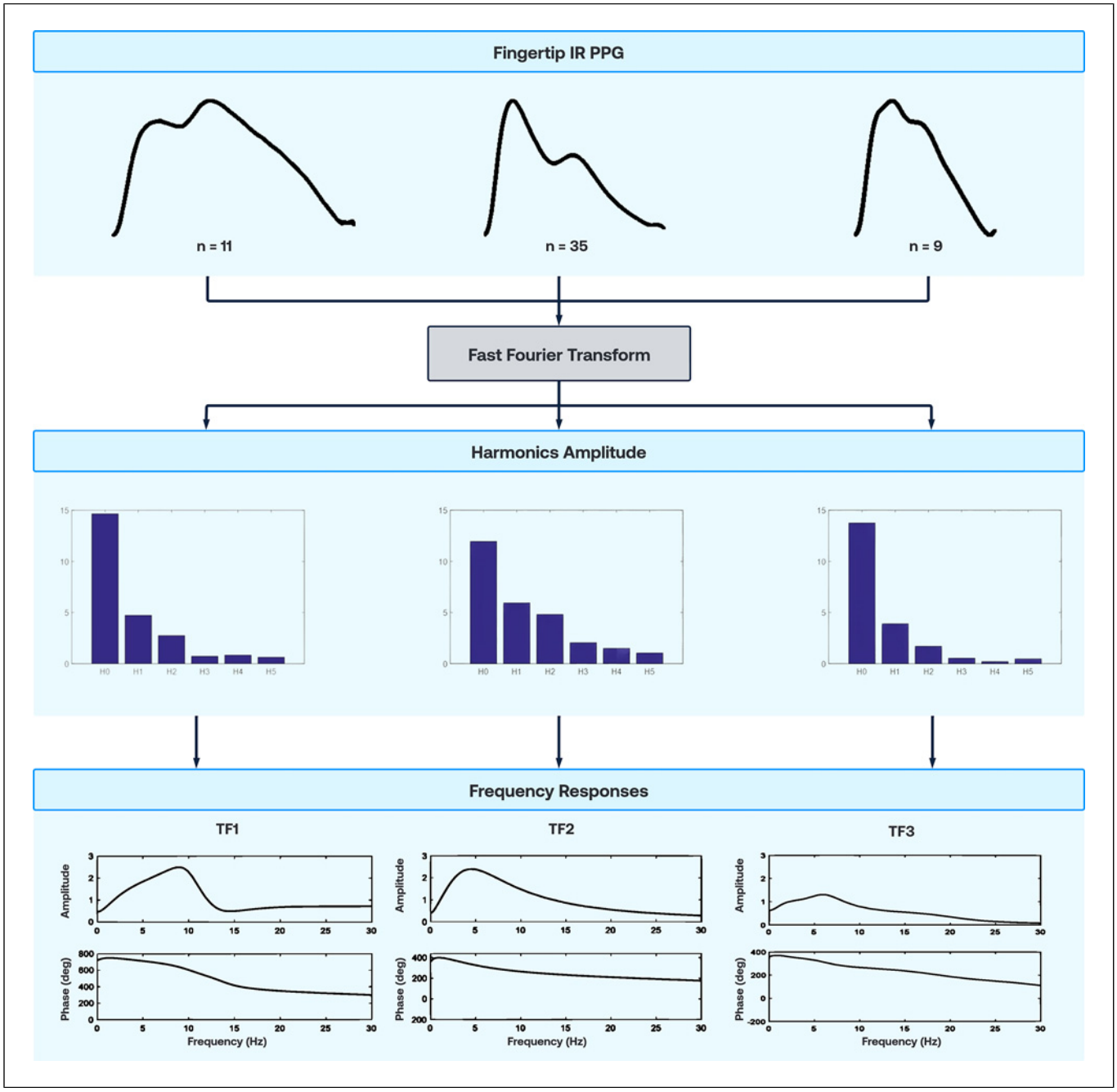


**Fig. 2.** Example of three types of fingertip IR PPG pulses with different harmonic profiles and the three corresponding fingertip IR PPG signals to radial pulse TFs (TF 1, TF 2, and TF 3). TF 1, first TF 1; TF 2, second TF 2; TF 3, third TF 3.

central to peripheral vasculature); HR (frequency of cardiac cycles in beats per minutes); central mean arterial pressure (mean pressure during the cardiac cycle); central mean systolic pressure (mean pressure during systole); central mean diastolic pressure (mean pressure during diastole); central tension-time index (amount of the cardiac work during systole); central diastolic time index (amount of the cardiac work during diastole); central period; central waveform timepoint T2 (T2: time when the fiducial point occurs during systole); end systolic pressure (pressure at the end of systole); central waveform height P1 (P1: peak pressure of the forward traveling wave generated during cardiac ejection); central waveform height P2 (P2: pressure of the reflected traveling wave caused by impedance mismatch during systole); and ejection duration (ED: percentage [or time] of the cardiac cycle spent during systole).

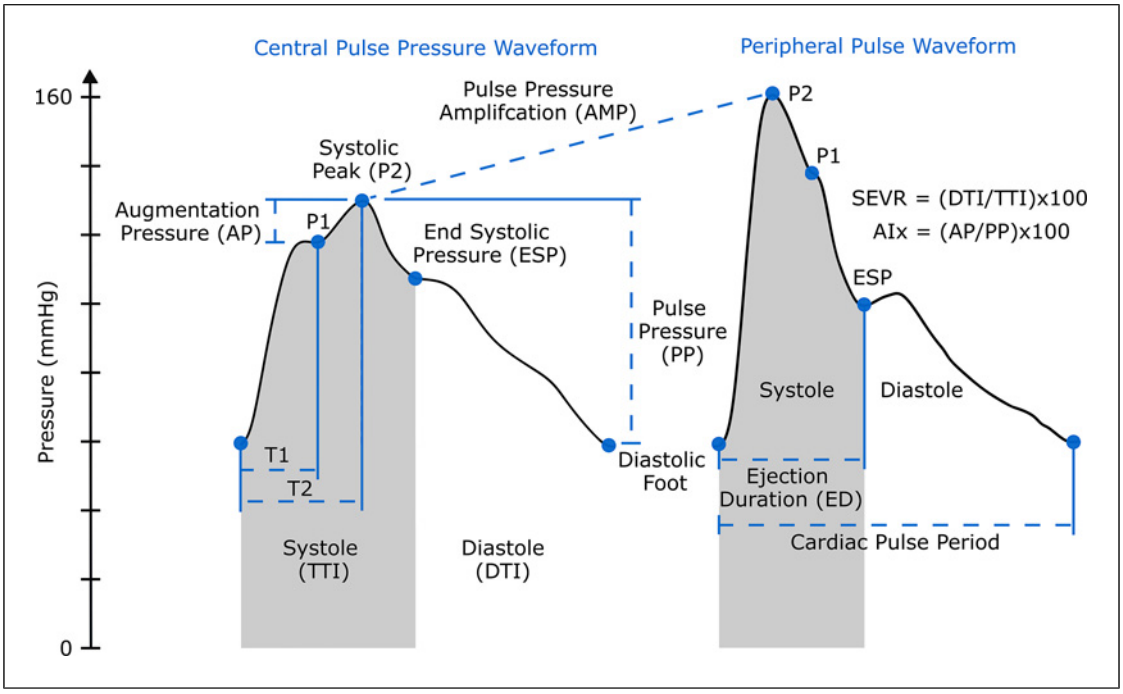


**Fig. 3.** Annotated central aortic pulse pressure waveform and peripheral pulse (e.g., radial artery) waveform. AIx, augmentation index; DTI, diastolic time index; SEVR, subendocardial viability ratio; and TTI, tension-time index.

*Statistical Analysis*

Analyses were conducted using Python (version 3.11.2). All central PWA parameters were compared through correlation analysis and using Bland-Altman plots. Significant differences were compared using a mixed-effects repeated measures ANOVA approach and deemed statistically significant where $p < 0.05$ with differences described as mean ± standard deviation. Peripheral and central aortic waveform shape, as generated using the respective TFs, was compared with root-mean-squared error (RMSE) as a percentage. The same RMSE analysis was also performed on just the systole and diastole sections of the waveform separately. No analysis of potential sex or age differences was performed.

**Table 1.** Participant demographics ($n$ = 21, 10 females)

| Parameter | Mean±SD | Range |
|---|---|---|
| Brachial SBP, mm Hg | 121±13 | 92–139 |
| Brachial DBP, mm Hg | 75±10 | 53–94 |
| Age, years | 39±16 | 19–74 |
| Height, cm | 173±11 | 155–195 |
| Weight, kg | 72±14 | 55–106 |
| Body mass index, kg/m$^2$ | 24±3 | 20–30 |

DBP, diastolic blood pressure; SBP, systolic blood pressure; SD, standard deviation.

## Results

Twenty-one healthy participants were included in this study ($n$ = 21, 10 females, age: 39 ± 16 years). Participant demographics are shown in Table 1. An example of the peripheral and aortic waveforms for the three subtypes of waveforms derived from both the radial tonometric reference and fingertip PPG is provided in Figure 4. From the 55 fingertip IR PPG measurements tested, a total of 11 measurements were converted to radial waveform using the first TF, 35 converted with the second TF (TF 2), and 9 converted with the third TF (TF 3) demonstrating a trend toward a normal distribution (shown in Fig. 2). Comparison of centrally derived waveform parameters for the radial tonometry and fingertip PPG technique is summarized in Table 2. This contains both calibrated (pressure-dependent) and uncalibrated (pressure-independent) waveform parameters. Correlation (r) between all parameters, regardless of pressure dependency, ranged from 0.79 to 0.99. Despite differences of some pressure-dependent parameters being statistically significant, these differences were not physiologically meaningful considering all pressure-based parameters had differences ranging between 0.2 and 1.3 mm Hg.

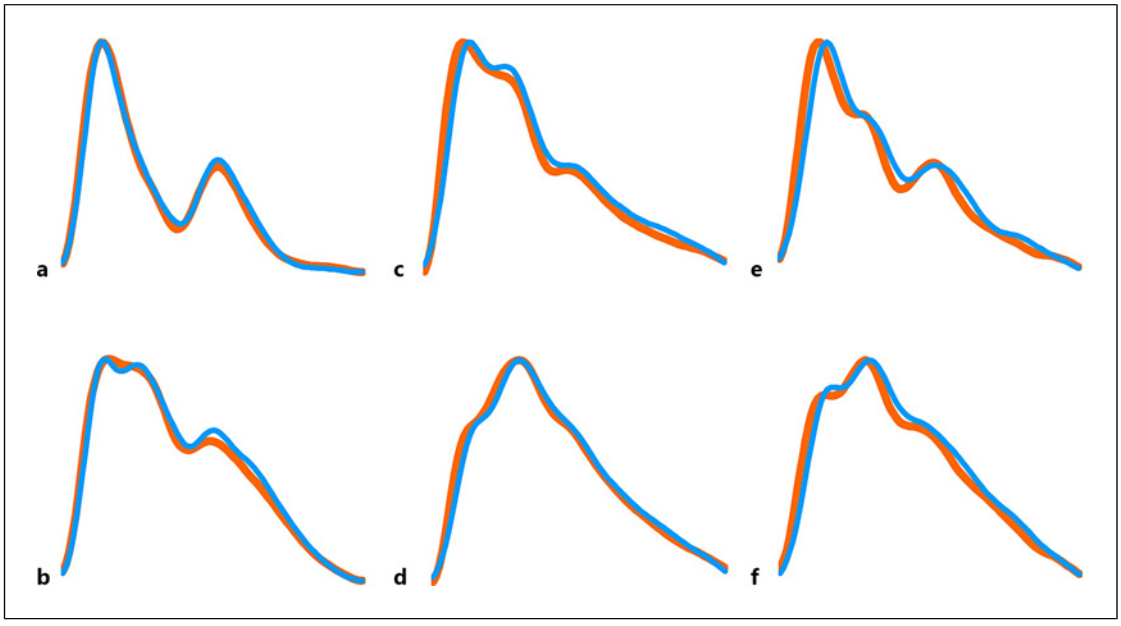


**Fig. 4.** Example of three different peripheral radial waveforms (**a**, **c**, **e**) and their derived central aortic pressure waveforms (**b**, **d**, **f**) from radially tonometry (orange) and PPG converted to radial waveforms (blue).

**Table 2.** Comparison of centrally derived aortic waveform parameters

| PWA Parameters | SphygmoCor CVMS | Fingertip PPG | Correlation *r* | Difference | *p* value |
|---|---|---|---|---|---|
| cSBP, mm Hg | 109±12 | 108±13 | 0.99 | 0.7±2.0 | **0.028** |
| cDBP, mm Hg | 77±9 | 76±9 | 0.99 | 0.4±1.1 | **0.004** |
| cPP, mm Hg | 32±6 | 32±7 | 0.96 | 0.2±2.0 | 0.325 |
| cAP, mm Hg | 5±5 | 5±5 | 0.94 | 0.4±1.8 | 0.181 |
| cAIx, % | 14±13 | 13±13 | 0.95 | 1.5±4.1 | 0.106 |
| cAIx75, % | 12±13 | 11±13 | 0.95 | 1.7±4.1 | 0.063 |
| SEVR, % | 165±25 | 163±34 | 0.88 | 1.7±16.4 | 0.453 |
| AMP, % | 147±19 | 149±22 | 0.91 | −2.2±9.3 | 0.122 |
| HR, bpm | 71±9 | 71±9 | 0.98 | 0.4±1.6 | 0.122 |
| cMAP, mm Hg | 92±10 | 91±10 | 0.97 | 0.8±2.6 | **0.024** |
| cMPS, mm Hg | 101±10 | 99±11 | 0.99 | 1.3±1.7 | <**0.001** |
| cMPD, mm Hg | 87±9 | 86±10 | 0.95 | 0.7±3.0 | 0.111 |
| cTTI, mm Hg.s | 2,096±288 | 2,103±330 | 0.94 | −7±111 | 0.625 |
| cDTI, mm Hg.s | 3,402±400 | 3,347±419 | 0.95 | 55±130 | **0.002** |
| cPeriod, ms | 861±125 | 865±120 | 0.99 | −4.1±17.8 | 0.295 |
| T2, ms | 207±207 | 214±12 | 0.79 | −7.1±11.7 | <**0.001** |
| ESP, mm Hg | 101±11 | 101±13 | 0.95 | 0.4±4.1 | 0.422 |
| P1, mm Hg | 104±10 | 103±10 | 0.99 | 0.3±1.3 | 0.098 |
| P2, mm Hg | 109±12 | 108±13 | 0.99 | 0.9±2.2 | **0.011** |
| ED, % | 35±4 | 35±4 | 0.91 | −0.5±1.7 | **0.037** |

Data presented as mean ± SD. cAIx, central augmentation index; AMP, pulse pressure amplification; cAP, central augmentation pressure; cDBP, central diastolic blood pressure; cDTI, central diastolic time interval; ED, ejection duration; ESP, end systolic pressure; HR, heart rate; cMAP, central mean arterial pressure; cMPD, central mean diastolic pressure; cMPS, central mean systolic pressure; PWA, pulse wave analysis; cPP, central pulse pressure; PPG, photoplethysmography; cSBP, central systolic blood pressure; SD, standard deviation; cTTI, central tension-time index; cAIx75, central augmentation index corrected to a heart rate of 75 beats per minute.

**Table 3.** Comparison of waveform shape

| Waveform section | RMSE, % | | |
|---|---|---|---|
| | mean±SD | minimum | maximum |
| Peripheral waveform | 2.8±1.2 | 0.9 | 7.2 |
| Peripheral systole | 3.3±1.4 | 0.4 | 6.7 |
| Peripheral diastole | 2.3±1.3 | 0.4 | 7.6 |
| Central waveform | 1.8±0.9 | 0.6 | 4.4 |
| Central systole | 1.6±0.7 | 0.4 | 3.4 |
| Central diastole | 1.8±1.1 | 0.5 | 5.0 |

RMSE, root-mean-squared error; SD, standard deviation.

Differences (RMSE) in waveform shape are summarized in Table 3. Differences in the waveform shape (illustrated in Fig. 4) were consistently low with diastole contributing to the largest variance in the central pressure waveform (1.8 ± 1.1%) and systole for the peripheral waveform (3.3 ± 1.4%).

Figure 5 displays the regression and Bland-Altman plots for the most commonly used aortic parameters from the peripherally derived central waveform. Calculated parameters using the novel selective TF tended to follow the line of unity (dotted line), as quantified by $r \geq 0.79$. As observed in the Bland and Altman plots (shown in Fig. 5), differences in parameters were mostly within their respective confidence intervals (cSBP CI: −3.2 to 4.5 mm Hg; cAIx corrected to a HR of 75 beats per minute CI: −6.3 to 9.8%; SEVR CI: −30.4 to 33.8%; and ED CI: −3.8 to 2.7%) with the largest variance observable in SEVR (refer to the SDs in Table 2).

## Discussion

Both pressure-calibrated and pressure-uncalibrated central aortic waveform parameters were successfully derived from a fingertip PPG sensor using a novel selective TF and were comparable to parameters derived from radial tonometry (noninvasive reference). As quantifiable from the mean differences in Table 2 and the confidence limits observable in the Bland-Altman plots (shown in Fig. 5), all pressure-based parameters were within 1.3 mm Hg, with cSBP and cDBP within the acceptable limits of 5 ± 8 mm Hg, with the proviso being that the sample size and demographics in this study are not as specified in the standards for BP device testing [23]. Similar to pressure-dependent parameters, the pressure-independent parameters had high correlation values with minimal mean differences.

It should be noted that the high correlations observed are in part due to the measured and the converted radial waveforms being calibrated with the same systolic and diastolic BP values. The similarity of the uncalibrated waveforms was the focus of this study, i.e., converting the measured fingertip IR PPG waveform to a radial waveform that is similar to the measured radial tonometric waveform (reference). Differences observed between estimates of central aortic waveform parameters therefore likely stem from variations in the reconstructed radial pressure waveforms due to different measurement modalities, considering that the same GTF was used. As mentioned, this study utilizes a previously validated and proprietary algorithm for converting a radial pressure waveform into central aortic waveform. The applied TF has already shown equivalence between the radial tonometric waveform and its invasive counterpart as well as being rigorously tested (FDA approval), invasively validated and accepted [11]. Thus, if we can successfully convert the fingertip PPG signal into a radial pressure waveform, as performed in this study, there is no need to generate a direct TF between the fingertip PPG and central aortic waveform, which would require further invasive studies to be undertaken. In continuation from this point, the findings give confidence in using fingertip PPG waveforms to derive central aortic waveforms for subsequent PWA of aortic waveforms. This modality of pulse acquisition has value in an ambulatory setting due to the convenience and comfort of measurements achievable with a PPG sensor. PPG measurement also allows increased frequency of measurement, which has the capacity to provide additional insight into an individual's cardiovascular profile beyond conventional BP measurements.

The comparisons made in this study included a diverse selection of 20 different PWA parameters. The parameters included in this study encapsulate an assortment of features representative of various waveform components, i.e., pressure-dependent and pressure-independent parameters, waveform shape parameters based on areas and fiducial points, and parameters associated with both the systolic and diastolic portions of the waveform. While diverse, this is limited such that it only includes a selection of parameters that have previously been calculated and assessed using the proprietary SphygmoCor software. There is a surplus of alternate parameters that may be incorporated in PWA such as the reflection index [24] or vascular age [25]. The clinical relevance of these parameters has been previously summarized in the literature [15, 26]. The inclusion of a wider selection of these parameters may further enhance the PWA assessment

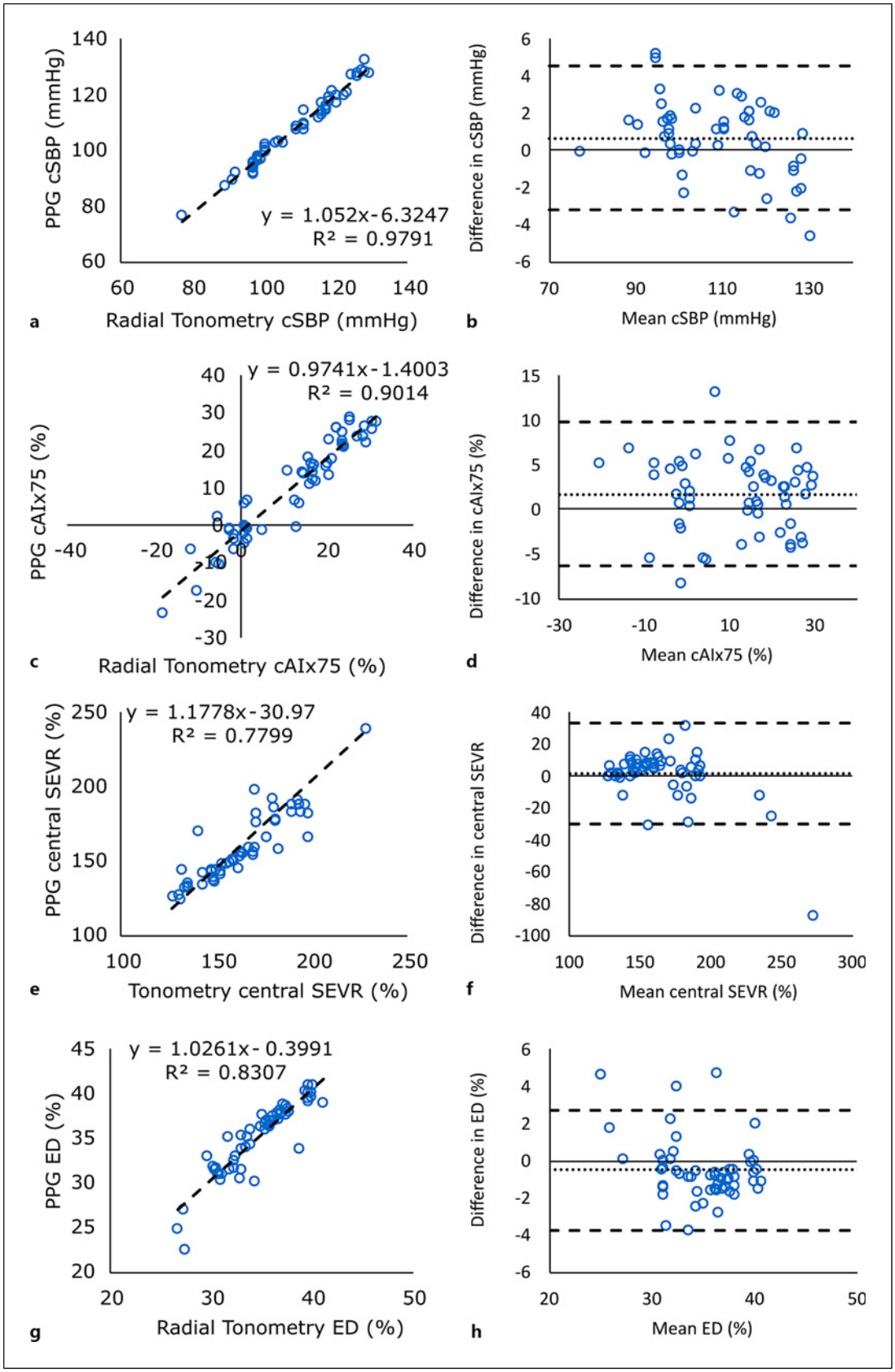


**Fig. 5.** Regression and Bland-Altman plots of central aortic waveform parameters. **a**, **b** cSBP. **c**, **d** cAIx75. **e**, **f** SEVR. **g**, **h** ED. cAIx75, central augmentation index corrected to a heart rate of 75 beats per minute; ED, ejection duration.

providing additional insight as to what parameters change under certain physiological conditions or diseases. However, despite not calculating these additional parameters the selection included in this study highlights that the waveform shape can already be reliably depicted, thus giving confidence that alternative waveform parameters may successfully be calculated.

Female menstrual cycle was not standardized in this study. While estradiol has been shown that it can impact the arterial waveform [27], differences across females due to this result in a wider variety of waveform shapes which again supports the reliability showing that the TFs are applicable across a more diverse cohort.

Interindividual waveform variability is another consideration when undertaking PWA and in the application of TFs. While an assortment of waveform shapes was captured (presented in Fig. 4) which displayed population variance of harmonic profiles (shown in Fig. 2), assessment of the novel selective TF would benefit from an investigation in individuals with cardiovascular-based diseases and complications known to influence the arterial waveform shape, such as hypertensives or individuals with heart abnormalities [28–30]. This would enhance the clinical relevance of performing PWA in individuals across the entire population acting as technology that aids in monitoring and management. Following from this, it is important to also consider that measurement of these central aortic parameters is intended for resting baseline conditions. While the measurement of central aortic PWA under dynamic conditions has previously been performed [31], this particular study employed the use of the GTF using radial tonometry and not PPG. As the sensor modality and TFs are fundamentally different between radial tonometry and fingertip PPG, the same conclusion cannot be made regarding the use of this novel selective TF.

Irrespective of sensor modality, discrepancies may arise in the presence of motion, which can be user dependent or independent. PPG measurements in particular are known to be prone to such noise which becomes amplified, especially during exercise. In addition, any form of exercise, static or dynamic, will result in blood volume changes to meet metabolic demands. As PPG is an optical-based sensor that measures changes in arterial blood volume, it is possible that exercise may influence the waveform through local blood perfusion changes. Other modalities, such as tonometry (force-based), may not be as sensitive in detecting these changes resulting in a slightly different waveform shape, and consequently the derived central aortic waveform and its accompanying parameters. These differences may further manifest following changes in vasomotor tone (vasoconstriction and vasodilation). Studies have previously shown that when undertaking interventions that impact the vasomotor sensitivity differences in waveform features, such as the pulse transit time, may differ across sensor modalities [32, 33]. This highlights the need for standardization of measurement acquisition.

In conclusion, the use of the fingertip PPG for waveform acquisition to derive central aortic PWA parameters has the capacity to broaden our assessment of an individual's cardiovascular profile. Assessment of these parameters under altered conditions holds merit for the assessment of other cardiovascular-based components, such as cardiorespiratory fitness or other stressor responses [34, 35], but further investigation is required. This study demonstrates that the fingertip PPG has capability of deriving aortic PWA parameters under controlled conditions.


## Acknowledgments

The authors would like to thank all participants who contributed toward this work.


## Statement of Ethics

This study was reviewed and approved by Macquarie University Human Ethics Research Committee, Approval No. 52022911840017. Participants provided written informed consent.

## Conflict of Interest Statement

J.R.C. and G.J.B. are sponsored by, A.P.A. is on the advisory board of, and E.A., C.L., and A.Q. are employees of Cardiex Limited.


## Funding Sources

This study was not supported by any sponsor or funder.


## Author Contributions

The following outlines the contributions made by the listed authors: J.R.C. contributed toward attaining the ethics, the generation of the protocol, and collection and analysis of data, and was involved in the writing and publication of this work; E.A. processed all the de-identified data generating the waveform parameters; A.P.A. provided technical expertise and guidance throughout the project and through reviewing of the manuscript; M.B. contributed toward acquiring the ethics, overseeing the collection and storage of data as well as critically reviewing the

manuscript; C.L. was involved with reviewing the manuscript and dissemination of the findings; G.J.B. was involved with reviewing the manuscript and the presentation of findings; and A.Q. was involved with the protocol development, the generation and development of the TFs used for waveform analysis, and the reviewing and dissemination of this work.

## Data Availability Statement

All data generated or analyzed during this study are included in this article. TFs applied to the measured waveforms involve the use of proprietary technology and will not be made publicly available. Further inquiries can be directed to the corresponding author.

## References


1 Glynn RJ, L'Italien GJ, Sesso HD, Jackson EA, Buring JE. Development of predictive models for long-term cardiovascular risk associated with systolic and diastolic blood pressure. Hypertension. 2002;39(1):105–10. https://doi.org/10.1161/hy1201.097199
2 Fuchs FD, Whelton PK. High blood pressure and cardiovascular disease. Hypertension. 2020;75(2):285–92. https://doi.org/10.1161/HYPERTENSIONAHA.119.14240
3 Dzau VJ, Balatbat CA. Future of hypertension. Hypertension. 2019;74(3):450–7. https://doi.org/10.1161/HYPERTENSIONAHA.119.13437
4 Phan K, Gomez YH, Gorgui J, El-Messidi A, Gagnon R, Abenhaim HA, et al. Arterial stiffness for the early prediction of pre-eclampsia compared with blood pressure, uterine artery Doppler and angiogenic biomarkers: a prospective cohort study. BJOG An Int J Obstet Gynaecol. 2023;130(8):932–40. https://doi.org/10.1111/1471-0528.17430
5 Salvi P, Valbusa F, Kearney-Schwartz A, Labat C, Grillo A, Parati G, et al. Non-invasive assessment of arterial stiffness: pulse wave velocity, pulse wave analysis and carotid cross-sectional distensibility: comparison between methods. J Clin Med. 2022;11(8):2225. https://doi.org/10.3390/jcm11082225
6 Salvi P, Baldi C, Scalise F, Grillo A, Salvi L, Tan I, et al. Comparison between invasive and non-invasive methods to estimate subendocardial oxygen supply and demand imbalance. J Am Heart Assoc. 2021;10(17):e021207. https://doi.org/10.1161/JAHA.121.021207
7 Charlton PH, Mariscal Harana J, Vennin S, Li Y, Chowienczyk P, Alastruey J. Modeling arterial pulse waves in healthy aging: a database for in silico evaluation of hemodynamics and pulse wave indexes. Am J Physiol Heart Circ Physiol. 2019;317(5):H1062–85. https://doi.org/10.1152/ajpheart.00218.2019
8 Roman MJ, Devereux RB, Kizer JR, Lee ET, Galloway JM, Ali T, et al. Central pressure more strongly relates to vascular disease and outcome than does brachial pressure: the strong heart study. Hypertension. 2007;50(1):197–203. https://doi.org/10.1161/HYPERTENSIONAHA.107.089078
9 Safar ME. Arterial stiffness as a risk factor for clinical hypertension. Nat Rev Cardiol. 2018;15(2):97–105. https://doi.org/10.1038/nrcardio.2017.155
10 Chen C-H, Nevo E, Fetics B, Pak PH, Yin FCP, Maughan WL, et al. Estimation of central aortic pressure waveform by mathematical transformation of radial tonometry pressure. Validation of generalized transfer function. Circulation. 1997;95(7):1827–36. https://doi.org/10.1161/01.cir.95.7.1827
11 Pauca AL, O'Rourke MF, Kon ND. Prospective evaluation of a method for estimating ascending aortic pressure from the radial artery pressure waveform. Hypertension. 2001;38(4):932–7. https://doi.org/10.1161/hy1001.096106
12 Hwang M-H, Yoo J-K, Kim H-K, Hwang C-L, Mackay K, Hemstreet O, et al. Validity and reliability of aortic pulse wave velocity and augmentation index determined by the new cuff-based SphygmoCor Xcel. J Hum Hypertens. 2014;28(8):475–81. https://doi.org/10.1038/jhh.2013.144
13 Benas D, Kornelakis M, Triantafyllidi H, Kostelli G, Pavlidis G, Varoudi M, et al. Pulse wave analysis using the Mobil-O-Graph, Arteriograph and Complior device: a comparative study. Blood Press. 2019;28(2):107–13. https://doi.org/10.1080/08037051.2018.1564236
14 O'Rourke MF, Pauca A, Jiang XJ. Pulse wave analysis. Br J Clin Pharmacol. 2001;51(6):507–22. https://doi.org/10.1046/j.0306-5251.2001.01400.x
15 Park J, Seok HS, Kim S-S, Shin H. Photoplethysmogram analysis and applications: an integrative review. Front Physiol. 2021;12:808451. https://doi.org/10.3389/fphys.2021.808451
16 Gallagher D, Adji A, O'Rourke MF. Validation of the transfer function technique for generating central from peripheral upper limb pressure waveform. Am J Hypertens. 2004;17(11 Pt 1):1059–67. https://doi.org/10.1016/j.amjhyper.2004.05.027
17 Avolio AP, Butlin M, Walsh A. Arterial blood pressure measurement and pulse wave analysis—their role in enhancing cardiovascular assessment. Physiol Meas. 2010;31(1):R1–47. https://doi.org/10.1088/0967-3334/31/1/R01
18 Shoji T, Nakagomi A, Okada S, Ohno Y, Kobayashi Y. Invasive validation of a novel brachial cuff-based oscillometric device (SphygmoCor XCEL) for measuring central blood pressure. J Hypertens. 2017;35(1):69–75. https://doi.org/10.1097/HJH.0000000000001135
19 Mallion JM, de GR, Baguet JP, Azzouzi L, Quesada JL, Sauzeau C, et al. Acceptability and tolerance of ambulatory blood pressure measurement in the hypertensive patient. Blood Press Monit. 1996;1(3):197–203.
20 Kyriacou PA, Allen J. Photoplethysmography: technology, signal analysis and applications. Academic Press; 2021.
21 Murgo JP, Westerhof N, Giolma JP, Altobelli SA. Aortic input impedance in normal man: relationship to pressure wave forms. Circulation. 1980;62(1):105–16. https://doi.org/10.1161/01.cir.62.1.105
22 Wilkinson IB, MacCallum H, Flint L, Cockcroft JR, Newby DE, Webb DJ. The influence of heart rate on augmentation index and central arterial pressure in humans. J Physiol. 2000;525 Pt 1(Pt 1):263–70. https://doi.org/10.1111/j.1469-7793.2000.t01-1-00263.x
23 Stergiou GS, Alpert B, Mieke S, Asmar R, Atkins N, Eckert S, et al. A universal standard for the validation of blood pressure measuring devices. Hypertension. 2018;71(3):368–74. https://doi.org/10.1161/hypertensionaha.117.10237
24 Ahn JM. New aging index using signal features of both photoplethysmograms and acceleration plethysmograms. Healthc Inform Res. 2017;23(1):53–9. https://doi.org/10.4258/hir.2017.23.1.53
25 Alastruey J, Charlton PH, Bikia V, Paliakaite B, Hametner B, Bruno RM, et al. Arterial pulse wave modeling and analysis for vascular-age studies: a review from VascAgeNet. Am J Physiol Heart Circ Physiol. 2023;325(1):H1–29. https://doi.org/10.1152/ajpheart.00705.2022
26 Suboh MZ, Jaafar R, Nayan NA, Harun NH, Mohamad MSF. Analysis on four derivative waveforms of photoplethysmogram (PPG) for fiducial point detection. Front Public Health. 2022;10:920946. https://doi.org/10.3389/fpubh.2022.920946
27 Seeland U, Demuth I, Regitz-Zagrosek V, Steinhagen-Thiessen E, König M. Sex differences in arterial wave reflection and the role of exogenous and endogenous sex hormones: results of the Berlin Aging Study II. J Hypertens. 2020;38(6):1040–6. https://doi.org/10.1097/HJH.0000000000002386
28 Weber T, Auer J, O'Rourke MF, Kvas E, Lassnig E, Berent R, et al. Arterial stiffness, wave reflections, and the risk of coronary artery disease. Circulation. 2004;109(2):184–9. https://doi.org/10.1161/01.CIR.0000105767.94169.E3
29 Nichols WW. Clinical measurement of arterial stiffness obtained from noninvasive pressure waveforms. Am J Hypertens. 2005;18(1 Pt 2):3S–10S. https://doi.org/10.1016/j.amjhyper.2004.10.009

30 Chirinos JA, Kips JG, Jacobs DR, Brumback L, Duprez DA, Kronmal R, et al. Arterial wave reflections and incident cardiovascular events and heart failure: MESA (Multiethnic Study of Atherosclerosis). J Am Coll Cardiol. 2012; 60(21):2170–7. https://doi.org/10.1016/j.jacc.2012.07.054
31 Sharman JE, Lim R, Qasem AM, Coombes JS, Burgess MI, Franco J, et al. Validation of a generalized transfer function to noninvasively derive central blood pressure during exercise. Hypertension. 2006;47(6): 1203–8. https://doi.org/10.1161/01.HYP.0000223013.60612.72
32 Di Rienzo M, Avolio A, Rizzo G, Zeybek ZMI, Cucugliato L. Multi-site pulse transit times, beat-to-beat blood pressure, and isovolumic contraction time at rest and under stressors. IEEE J Biomed Health Inform. 2022;26(2):561–71. https://doi.org/10.1109/JBHI.2021.3101976
33 Cox J, Avolio AP, Louka K, Shirbani F, Tan I, Butlin M. Blood pressure-independent neurogenic effect on conductance and resistance vessels: a consideration for cuffless blood pressure measurement? In: 2021 43rd annual international conference of the IEEE engineering in medicine & biology society. EMBC; 2021. p. 7485–8.
34 Fernberg U, Fernström M, Hurtig-Wennlöf A. Arterial stiffness is associated to cardiorespiratory fitness and body mass index in young Swedish adults: the Lifestyle, Biomarkers, and Atherosclerosis study. Eur J Prev Cardiol. 2017;24(17):1809–18. https://doi.org/10.1177/2047487317720796
35 Carlini NA, Cloud RMT, Harber MP, Fleenor BS. Cardiorespiratory fitness is associated with estimates of myocardial perfusion: influence of age and sex. Am J Physiol Heart Circ Physiol. 2024;326(1): H103–9. https://doi.org/10.1152/ajpheart.00610.2023